I-band Measurements of Red Giant Variables: Methods and Photometry of 66 Stars

Terry T. Moon
Sydney Institute for Astronomy, School of Physics, University of Sydney, NSW 2006, Australia

Received April 11, 2013; revised May 16, 2013; accepted May 16, 2013

Abstract New measurements of I_C and $V–I_C$ are presented for 66 bright red giant variables. This is the first stage of a program to measure sufficient numbers of such stars that also have well-determined Hipparcos parallaxes with a view to calibrating the TRGB in the I_C band as a tool for accurately measuring distances to nearby galaxies.

1. Introduction

The evolutionary paths of red giant variables follow a two-stage ascent on the HR diagram. In the first stage, they ascend the Red Giant Branch (RGB) burning hydrogen in a shell around the core. Their luminosity increases over time until they reach the point where helium burning commences. After the depletion of helium in the core, a second ascent on a parallel path, the Asymptotic Giant Branch (AGB), occurs. Measuring the end of the first ascent, that is, the Tip of the Red Giant Branch (TRGB), has been shown by Madore and Freedman (1995) to provide a means of determining the distance to nearby galaxies comparable in accuracy to using Cepheid variables. Through generating synthetic *I* magnitudes as a function of *V–I* color index (for Population II stars) their computer simulations indicated that this discontinuity as measured at *I*-band could be used as a primary distance indicator for galaxies to an accuracy of ±10% out to 3 Mpc.

The TRGB represents the maximum luminosity reached by red giants during their first ascent, and is associated with the sudden onset of helium burning in the core, providing a well-defined discontinuity that can be readily observed (Tabur *et al.* 2009a). As red giant variables are both bright and abundant, measurement of the TRGB offers both high utility for, and accuracy in, measuring cosmic distances. The TRGB method purportedly continues to grow in popularity owing to its "low cost in observing time, its conceptual simplicity, and its wide range of application" (Madore *et al.* 2009). Tabur *et al.* (2009a) extended the TRGB method to red giant variables in the solar neighbourhood using photometry from the 2MASS and DIRBE catalogs together with revised Hipparcos parallaxes. Madore *et al.* (2009) introduced a modified detection method for measuring the luminosity of the TRGB based on composite *I* magnitudes modified using a scaling of the *V–I* color index to account for known systematic variations due to metallicity.

For locating the TRGB, near-infrared—that is, *I*-band—measurements are preferred to measurements in other bands as:

- *I*-band magnitudes provide a better indicator of luminosity for red giants than *V* magnitudes. In M giants large variations in *V* arise from a substantial change in temperature as they pulsate. At their cooler phase, red giants emit a smaller fraction of their total energy in the visual portion of the spectrum. Additionally TiO molecules that form during the cooler phase absorb light preferentially in *V*-band (Percy 2007).
- Interstellar reddening corrections are reduced in the near infrared (Tabur *et al.* 2009a).
- *I*-band measurements are less sensitive to metallicity (Tabur *et al.* 2009a).

Additionally, Bedding (2009) has suggested that single-epoch *I*-band measurements may be sufficient to calibrate the TRGB as a tool for measuring cosmic distances.

Unfortunately there is a paucity of *I*-band measurements for those M giants with well-determined Hipparcos parallaxes (Tabur *et al.* 2009a). The available *I*-band data are a mixture of measurements using different systems. For the 261 M giants listed by Tabur *et al.* (2009b), the *General Catalogue of Photometric Data* (GCPD; Mermilliod *et al.* 1997) gives Johnson *I*-band (I_J) values for only 56 of them; 24 of these also have Cousins *I*-band (I_C) values listed. There are an additional 6 stars for which only Cousins values are available. For the remaining 199 bright M giants in this list no *I*-band values are given in the GCPD. A program of systematic *I*-band measurements of bright, nearby M giants was thus started.

2. Which *I*-band?

Bessell (2005) discusses the different *RI* systems that arose as extensions of the well-defined *UBV* photometric system. Early on, a variety of photomultiplier tube and filter combinations were used which gave rise to substantially different *R* and *I* bands. In particular the Johnson *R* and *I* bands (Johnson *et al.* 1967) had significantly longer effective wavelengths than those defined by Kron and Smith (1951) or Cousins (1976).

Precise southern *UBVRI* standards established by Cousins (1976, 1980) provided a good representation of the Johnson and Morgan *UBV* system (1953) and were related linearly to Kron's *RI* system (Kron and Smith 1951). As a result, the $UBV(RI)_C$ system emerged with well-defined passbands (Bessell 1979, 1990) and precisely measured standards (Menzies *et al.* 1989). This instantiation of a *UBVRI* system has been extended to CCD photometry (Bessell 1995), becoming the modern standard in which many new *UBVRI*

measurements are made. It was thus decided that near-infrared measurements of the M giants listed by Tabur *et al.* (2009b) would be made in the Cousins *I*-band (I_C).

3. Equipment

3.1. Photometers and telescopes

An Optec SSP-3 (Gen 1) photometer (Persha and Sanders 1983) was used for measuring about fifty of the brighter M giants listed by Tabur *et al.* (2009b). As this is a solid-state photometer with a photodiode detector it is less sensitive than photometers with photomultiplier tubes or those based on CCD cameras. It does, however, have a relatively good sensitivity in the near-infrared. Measurement methods followed were those suggested in the SSP-3 manual (Optec 2006).

For other M giants in the list of Tabur *et al.* (2009b), a system using a Meade DSI Pro II camera with its supplied software (Meade 2005) was developed. To use it as a photometer a filter wheel and a flip-mirror assembly with an illuminated-reticle eyepiece were added. A cooling fan was also attached. For data acquisition and processing, the techniques described by Hopkins and Lucas (2007) are followed. Telescopes used include a 15-cm f/12 Maksutov (for the SSP-3 photometer and Meade camera) and 12-cm f/5 and 7-cm f/7 refractors (camera only). All three telescopes are operated on equatorial mounts so as to avoid field rotation during CCD measurements.

3.2. Filters

Unfortunately the red and infrared filters originally supplied with the SSP-3 match the Johnson *RI* system. As the focus was on measuring I_C and $V - I_C$, a spare filter slide was fitted with the supplied Optec *V* filter and an I_C filter constructed using a Hoya RT-830 filter cemented between two optically-flat borosilicate windows (used as fill glass to bring the filter to the same thickness as the supplied *V* filter). As shown in Figure 1, the Hoya RT-830 filter has essentially the same spectral transmission characteristics as a Schott RG9, which is the filter usually specified for I_C band measurements (Bessell 1995).

The differences may be regarded as minor when it is noted that a filter's spectral transmission varies with changes in temperature (Young 1967) and, even for a specific filter make and type, from one manufactured batch to another. Subsequent measurements of standard stars over 24 nights confirmed that measurements made through this filter can be linearly transformed to standard I_C magnitudes and $V - I_C$ colors.

The advantage of the I_C filter described is that it is made from inexpensive and readily-available components supplied (such as by Edmunds Scientific) in a diameter that fits SSP-3 filter slides. For convenience (that is, having one of

the SSP-3's two-filter slides fitted with *B* and *V* filters and another with *V* and *I*) a new V filter was subsequently purchased. The new *V* filter was used for all $V–I_C$ measurements taken after July 30, 2011. For the Meade camera a larger diameter of the same type of Hoya filter was used but without the fill glass. For the *V*-filter an inexpensive Wratten #12 long-pass filter of the type supplied for visual astronomy applications (similar to Schott GG495) was cemented to a Schott BG39 visual band-pass filter.

4. Reduction and transformation of measurements

4.1. Standard stars

The standard stars chosen for calibrating the VI_C system described above were selected from the list of Menzies *et al.* (1989). For measurements with the less sensitive SSP-3 photometer attached to small telescopes only bright stars (Hoffleit and Warren 1991) can be used. This limits the choice of standard stars from the list of Menzies *et al.*, making it sometimes difficult to select standard stars with a wide spread of colors that could, at the time of observing, be measured at low air masses. The use of other bright stars as secondary standards was thus investigated.

Mean values of *V*, *B–V*, and *U–B* can be readily retrieved from the GCPD. For many bright stars such values are weighted means derived from multiple sources. Of the standards listed by Menzies *et al.* (1989), 100 are also listed as bright stars by Hoffleit and Warren (1991). Figure 2 shows that there is an excellent correspondence between the GCPD and Menzies *et al.* values for *V*, *B–V*, and *U–B*, with no apparent systematic variations with color index. The average difference between the GCPD and Menzies *et al.* (1989) values for the *V* band and *B–V* and *U–B* color indices were 0.001, 0.000, and –0.001, respectively, with standard deviations of 0.007, 0.003, and 0.005.

There are fewer sources of $V–R_C$ and $V–I_C$ colors and the GCPD lists individual values from each source rather than a weighted mean. Where the star is also a standard, its value given by Menzies *et al.* (1989) is listed separately in the GCPD and denoted as "STD." These standard values were not included in the values adopted from the GCPD for this analysis. Where there were multiple values the mean was calculated. Figure 3 shows the difference between GCPD and Menzies *et al.* (1989) values of $V–R_C$ and $V–I_C$ for those $UBV(RI)_C$ standards that are also bright stars. Again there is excellent agreement. For the $V–R_C$ and $V–I_C$ color indices the average difference between GCPD and standard values was +0.001, with a standard deviation in both cases of 0.002. It is, however, noted that some of the GCPD values are measurements by Cousins and co-workers.

For measurements of I_C and $V–I_C$ it is concluded that GCPD values for bright stars can be used as secondary standards.

4.2. Transformation to I_C and $V–I_C$

Atmospheric extinction coefficients were measured on most nights and applied to the data on a night-by-night basis. Average values for the atmospheric extinction coefficients measured on 24 nights (spread across seasons) were 0.20 and 0.12 for the V and I_C bands, respectively, which are in good agreement with mean values given by Allen (1973), Cousins (1976), Minniti *et al.* (1989), and Sung and Bessell (2000). The average value for I_C-band atmospheric extinction was used on those few nights for which no suitably accurate determination was made. (For the smaller number of CCD measurements average extinction coefficients were used.)

As shown in Figure 4, a linear relationship suffices for transforming the instrumental ($v–i$) indices measured with the SSP-3 photometer to standard $V–I_C$ colors. A small difference in the transformation constant does, however, occur from one V filter to another. Preliminary calibrations show that similar linear relationships apply to V and I_C magnitudes and the $V–I_C$ color index when using the CCD camera.

Measurements of M giants were made relative to selected comparison stars. In most cases the comparison stars used were the same as used previously by the author (see Tabur *et al.* 2009b). Typically, a chosen comparison star was close in the sky to the M giant and measured just before or just after it, keeping corrections for air mass differences to a minimum. An average value of the coefficient for transforming i to I_C magnitudes sufficed as comparison stars chosen were typically late K giants, minimizing the magnitude of the color corrections applied.

5. New I_C and $V–I_C$ measurements of red giant variables

Table 1 lists the new measurements made. Some stars were measured on more than one night to test the suggestion that single-epoch I-band measurements may be sufficient. Measurements made with the SSP-3 photometer are shown in normal type while recent CCD measurements are in italics. In the bottom portion of the table are measurements of several southern, bright M giants that are not included in the list of Tabur *et al.* (2009b). All but one of these is listed in the Hipparcos catalogue.

Of the M giants measured, seventeen have Cousins $V(RI)_C$ values listed in the GCPD. Using the forty-eight measurements of these seventeen stars, an average difference between measured and listed values of +0.01 ±0.10 magnitude was calculated. Considering that all M giants vary in light to some extent, and standard magnitudes are determined through extrapolating transformations established for earlier-type stars, the agreement is good. Similarly, the colors measured deviated only a few hundredths of a magnitude from listed values, which is within known variations that occur for transforming measurements of M giants to the $UBV(RI)_C$ system (Moon *et al.* 2008). The magnitudes and colors

measured may thus be considered to have been well transformed to standard I_C and $V–I_C$ values.

The CCD measurements included are early results in the extension of this program to fainter magnitudes and were made at a new observing site (Scottsdale, Tasmania). They were transformed using a preliminary calibration based on only a dozen standard stars. Also, a series of measurements of BQ Oct on one night show a larger scatter than for the SSP-3 measurements. This may in part be due to inadequate flat-field corrections or the observing conditions on the night. More data will be acquired to better define the transformation coefficients and to understand variations in atmospheric extinction at the new site. The challenges of all-sky CCD photometry are discussed further in Hopkins and Lucas (2007).

6. Conclusion

A program is underway to make I_C band measurements of those bright red giant variables for which there are also well-determined Hipparcos parallaxes. New data for the brighter M giants in the list of Tabur *et al.* (2009b) were gathered that are well transformed to standard VI_C magnitudes and color. This provides a basis for further work to measure sufficient numbers of red giant variables (with known parallaxes) in an effort to calibrate the TRGB in the I_C band as a tool for accurately measuring distances to nearby galaxies.

7. Acknowledgements

The continued support of the Astronomical Society of South Australia is appreciated. In particular, thank you to the Instrument Officer, Blair Lade, for his repairs of and modifications to the SSP-3 photometer. Thanks also to Professor Tim Bedding, Head of School of Physics, University of Sydney, for suggesting this project and his continued support.

References

Allen, C. W. 1973, *Astrophysical Quantities*, 3rd ed., Univ. London, Athlone Press, London.

Bedding, T. 2009, private communication (email of August 21).

Bessell, M. S. 1979, *Publ. Astron. Soc. Pacific*, **91**, 589.

Bessell, M. S. 1990, *Publ. Astron. Soc. Pacific*, **102**, 1181.

Bessell, M. S. 1995, in *New Developments in Array Technology and Applications*, eds. A. G. D. Philip, K. A. Janes, and A. R. Upgren, IAU Symp. 167, Kluwer, Dordrecht, 175.

Bessell, M. S. 2005, *Annu. Rev. Astron. Astrophys.*, **43**, 293.

Cousins, A. W. J. 1976, *Mem. Roy. Astron. Soc.*, **81**, 25.

Cousins, A. W. J. 1980, *South African Astron. Obs. Circ.*, **1**, 234.
Hoffleit, D., and Warren, W. H., Jr. 1991, *The Bright Star Catalogue*, 5th rev. ed., online-only reference (http://cdsarc.u-strasbg.fr/viz-bin/Cat?V/50).
Hopkins, J. L., and Lucas, G. A. 2007, *AutoStar CCD Photometry* (http://www.hposoft.com), Hopkins Phoenix Observatory, Phoenix, AZ.
Johnson, H. L., Mitchell, R. I., and Latham, A. S. 1967, *Commun. Lunar Planet. Lab.*, **6**, 85.
Johnson, H. L., and Morgan, W. W. 1953, *Astrophys. J.*, **117**, 313.
Kron, G. E., and Smith, J. L. 1951, *Astrophys J.*, **113**, 324.
Madore, B. F., and Freedman, W. J. 1995, *Astron. J.*, **100**, 1645.
Madore, B. F., Mager, V., and Freedman, W. J. 2009, *Astrophys. J.*, **690**, 389.
Meade Instruments Corp. 2005, AUTOSTAR SUITE software, Version 3.0 (www.meade.com).
Menzies, J. W., Cousins, A. W. J., Banfield, R. M., and Laing, J. D. 1989, *South African Astron. Obs. Circ.*, **13**, 1.
Mermilliod, J. C., Hauck, B., and Mermilliod, M. 1997, *Astron. Astrophys., Suppl. Ser.*, **124**, 349 (*General Catalogue of Photometric Data (GCPD) II*, http://obswww.unige.ch/gcpd/gcpd.html).
Minniti, D., Clariá, J. J., and Gómez, M. N. 1989, *Astrophys. Space Sci.*, **158**, 9.
Moon, T. T., Otero, S. A., and Kiss, L. L. 2008, *J. Amer. Assoc. Var. Star Obs.*, **36**, 77.
Optec 2006, *Model SSP-3 Solid-State Stellar Photometer* (Technical Manual), Optec Inc., Lowell, MI.
Percy, J. R. 2007, *Understanding Variable Stars*, Cambridge Univ. Press, Cambridge.
Persha, G., and Sanders, W. 1983, in *Advances in Photoelectric Photometry, Vol. 1.*, eds. R. C. Wolpert, R. M. Genet, and J. Wolpert, Fairborn Observatory, Fairborn, OH, p.130.
Sung, H., and Bessell, M. S. 2000, *Publ. Astron. Soc. Australia*, **17**, 244.
Tabur, V., Bedding, T. R., Kiss, L. L., Moon, T. T., Szeidl, B., and Kjeldsen, H. 2009b, *Mon. Not. Roy. Astron. Soc.*, **400**, 1945.
Tabur, V., Kiss, L. L., and Bedding, T. R. 2009a, *Astrophys. J., Lett.*, **703**, L72.
Young, A. T. 1967, *Mon. Not. Roy. Astron. Soc.*, **135**, 175.

Table 1. Measurements of I_C and $V–I_C$ for bright red giant variables.

*Star**	*HIP*	*JD*	I_C	$V–I_C$
U Ant	51821	2455653.981	2.70	2.73
		2455675.998	2.73	2.73
OO Aps	74999	2455312.083	4.29	2.19
		2456217.926	4.53	2.28
		2456232.933	4.56	2.47
delta[1] Aps	80047	2455677.003	2.01	2.81
theta Aps	68815	2455654.081	1.33	4.27
		2455676.992	1.18	4.11
EN Aqr	102624	2455898.953	2.22	2.18
V626 Ara	86628	2455821.920	3.69	2.46
		2456241.942	3.78	2.52
V854 Ara	84105	2455821.928	3.46	2.43
		2456241.944	3.50	2.35
RV Cae	*20856*	*2456365.938*	*4.77*	*1.68*
V505 Car	51141	2455676.979	4.29	2.25
		2455968.990	4.38	2.23
		2456003.963	4.36	2.23
V744 Cen	66666	2455676.006	2.26	3.49
V763 Cen	56518	2455654.023	3.26	2.33
		2455675.971	3.32	2.38
2 Cen	67457	2455654.085	1.08	2.99
		2455676.073	1.04	3.06
AD Cet	1158	2455898.989	2.84	2.20
AE Cet	1170	2455923.969	2.44	1.98
AR Cet	9372	2455923.990	2.39	3.04
BL Cru	60781	2455676.038	2.51	2.97
		2456003.993	2.54	2.91
gamma Cru	61084	2455654.031	-0.72	2.32
		2455676.028	-0.77	2.37
		2456003.985	-0.75	2.34
R Dor	21479	2455577.003	0.16	5.01
		2455677.925	-0.04	5.13
		2455899.069	0.25	5.18
		2455996.963	-0.09	4.91
WZ Dor	23840	2455577.029	2.79	2.42
		2455676.939	2.80	2.47
		2455924.019	2.81	2.35
eta[2] Dor	29353	2455577.043	2.76	2.12
		2455676.922	2.79	2.17
		2455923.053	2.85	2.12

Table 1 continued on following pages

Table 1. Measurements of I_C and $V–I_C$ for bright red giant variables, cont.

*Star**	*HIP*	*JD*	I_C	$V–I_C$
DM Eri	21763	2455923.019	2.03	2.27
		2455941.028	2.01	2.27
		2455996.933	1.85	2.30
FH Eri	*12016*	*2456259.976*	*4.36*	*2.73*
		2456312.022	*4.31*	*2.71*
tau[4] Eri	15474	2455923.003	1.24	2.36
		2455941.019	1.25	2.35
		2456003.926	1.27	2.41
DL Gru	114407	2455478.976	3.29	2.65
		2455801.021	3.31	2.51
		2455940.967	3.27	
beta Gru	112122	2455478.940	-0.61	2.77
		2455800.997	-0.56	2.58
		2455822.041	-0.60	2.69
delta[2] Gru	111043	2455470.940	1.61	2.51
		2455478.933	1.61	2.55
		2455801.005	1.63	2.51
		2455822.034	1.62	2.53
		2455898.969	1.60	2.43
pi[1] Gru	110478	2455478.958	1.88	4.72
		2455822.024	1.69	4.44
TV Hor	*11648*	*2456312.012*	*3.98*	*2.67*
TW Hor	14930	2455941.008	3.27	2.46
TZ Hor	11293	2455822.010	3.49	2.92
		2455899.051	3.47	2.88
		2455924.010	3.49	2.86
WX Hor	*17889*	*2456312.028*	*3.75*	*3.09*
gamma Hyi	17678	2455923.042	1.33	1.91
		2455940.988	1.31	1.91
		2456003.934	1.30	1.95
T Ind	105334	2455800.977	3.71	2.25
WX Men	26169	2455676.961	3.21	2.52
		2455969.000	3.29	2.57
		2455996.972	3.25	2.46
BO Mus	61404	2455676.047	2.29	3.55
epsilon Mus	59929	2455654.052	1.25	2.92
		2455676.064	1.28	2.92
V367 Nor	79490	2455677.038	3.74	2.08
		2455821.913	3.76	2.14
		2456232.944	3.75	2.37

Table 1 continued on following pages

Table 1. Measurements of I_C and $V–I_C$ for bright red giant variables, cont.

*Star**	*HIP*	*JD*	I_C	$V–I_C$
BQ Oct	*71348*	*2456232.970*	*4.29*	*2.60*
		2456319.987	*4.19*	*2.71*
		2456319.989	*4.20*	*2.70*
		2456319.990	*4.21*	*2.68*
		2456319.992	*4.23*	*2.68*
		2456319.992	*4.21*	*2.70*
		2456351.917	*4.12*	*2.70*
		2456351.918	*4.12*	*2.71*
		2456353.000	*4.20*	*2.64*
		2456354.951	*4.21*	*2.67*
		2456365.910	*4.27*	*2.72*
		2456382.887	4.16	2.75
epsilon Oct	110256	2455654.068	1.73	3.32
		2455677.903	1.78	3.30
		2455836.956	1.79	3.27
		2455925.036	1.77	3.26
omicron[1] Ori	22667	2455923.028	2.14	2.56
Y Pav	105678	2455821.975	3.62	2.70
		2455836.947	3.59	2.62
SX Pav	106044	2455821.971	2.15	3.24
		2455836.940	2.22	3.40
		2455924.992	2.09	3.17
NU Pav	98608	2455492.960	1.66	3.73
		2455821.958	1.65	3.62
		2455836.913	1.61	3.49
omicron Pav	104755	2455836.931	3.05	2.02
		2455924.985	3.02	1.99
SW Pic	28596	2455940.997	3.73	2.67
		2456303.997	4.00	2.35
WW Pic	*24943*	*2456382.920*	*4.44*	*2.14*
AC Pic	*30237*	*2456354.987*	*4.73*	*2.14*
TV Psc	2219	2455898.999	2.42	2.50
YY Psc	154	2455898.960	1.99	2.42
57 Psc	3632	2455923.981	2.71	2.52
AL Phe		*2456301.994*	*5.23*	*3.10*
		2456352.919	*5.26*	*2.86*
		2456352.949	*5.25*	*2.88*
AW Phe	*6952*	*2456301.986*	*3.63*	*2.65*
BU Phe	*3894*	*2456311.964*	*4.54*	*2.55*
		2456312.004	*4.58*	*2.48*

Table 1 continued on next page

Table 1. Measurements of I_C and $V–I_C$ for bright red giant variables, cont.

*Star**	*HIP*	*JD*	I_C	$V–I_C$
psi Phe	8837	2455478.999	1.88	2.56
		2455576.979	1.88	2.48
		2455821.999	1.90	2.41
l[2] Pup	34922	2455675.915	2.96	3.41
		2455925.049	3.14	3.05
		2455968.969	3.21	3.60
		2456003.949	3.40	4.07
gamma Ret	18744	2455576.953	2.01	2.44
		2455677.933	2.03	2.45
		2455899.062	1.97	2.40
X TrA	74582	2455312.075	3.01	2.45
		2455677.022	2.85	2.74
		2456232.940	3.02	2.99
BQ Tuc	4200	2455479.028	2.91	2.92
		2455899.021	2.89	2.81
		2455925.024	2.90	2.79
CC Tuc	4879	2455899.028	3.97	2.24
		2455925.015	4.03	2.29
		2455940.979	4.02	2.31
CV Tuc	*3634*	*2456311.960*	*5.47*	*1.72*
		2456311.994	*5.45*	*1.74*
DR Tuc	115433	2455837.010	3.80	2.27
		2455925.004	3.82	2.25
nu Tuc	111310	2455478.968	2.36	2.49
		2455801.013	2.33	2.51
		2455821.991	2.41	2.47
		2455836.922	2.37	2.51
HR 935	14456	2455924.000	2.90	2.33
		2455968.960	2.91	2.30
HD 31754	*22737*	*2456365.945*	*4.92*	*1.49*
HD 33116	*23653*	*2456365.983*	*4.46*	*1.90*
HD 46742	*31221*	*2456354.924*	*5.77*	*2.21*

**Note: Stars having CCD measurements are given in italics.*

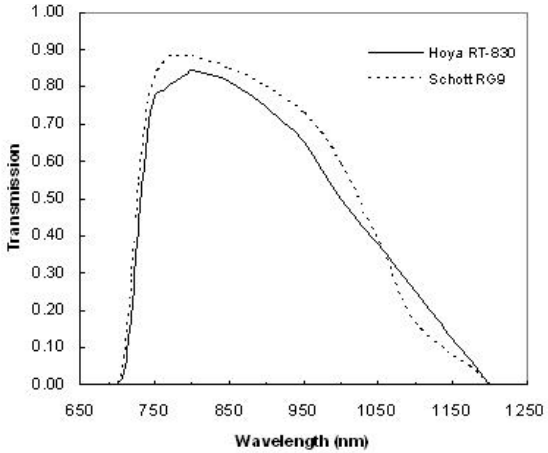

Figure 1. Spectral transmission of the Hoya RT-830 filter compared to a Schott RG9.

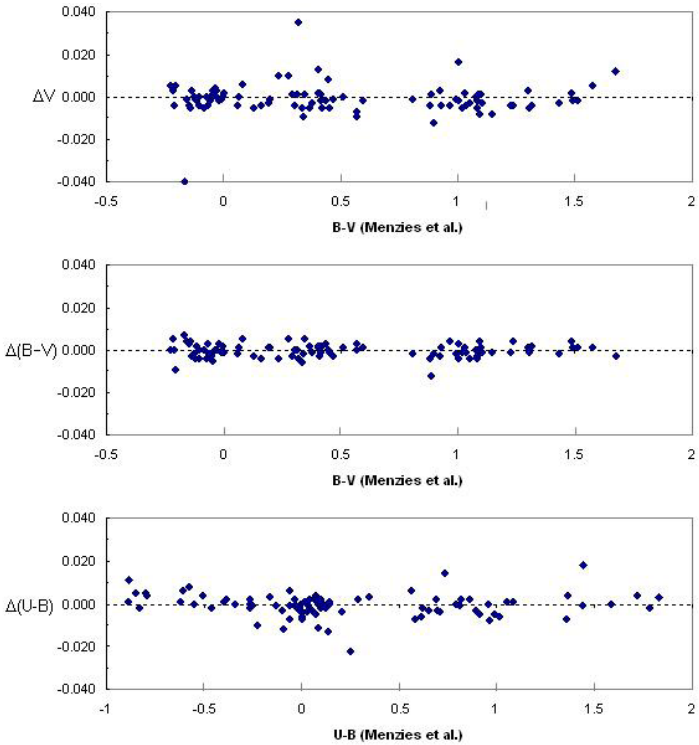

Figure 2. The differences between GCPD (Mermilliod *et al.* 1997) and Menzies *et al.* (1989) *V*, *B–V*, and *U–B* values as a function of the Menzies *et al. B–V* and *U–B* color indices.

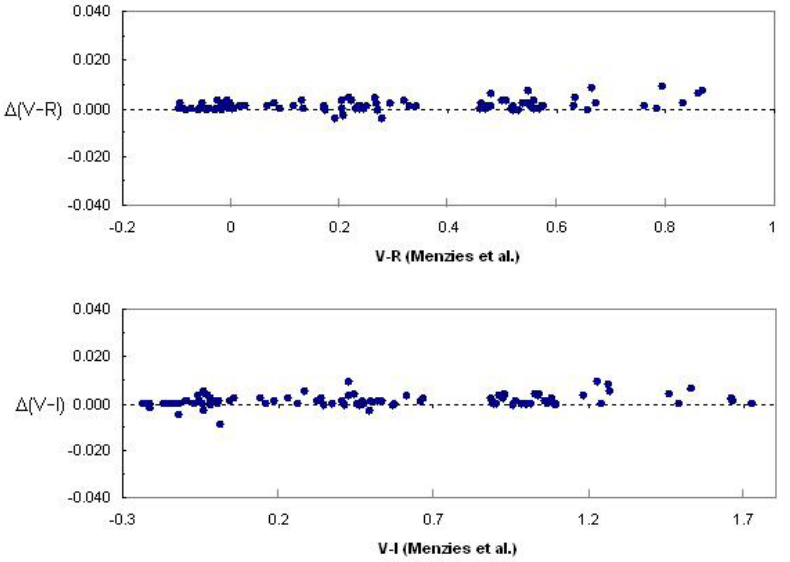

Figure 3. The differences between GCPD (Mermilliod *et al.* 1997) and Menzies *et al.* (1989) $V–R_C$ and $V–I_C$ values as a function of the Menzies *et al.* and $V–I_C$ color indices.

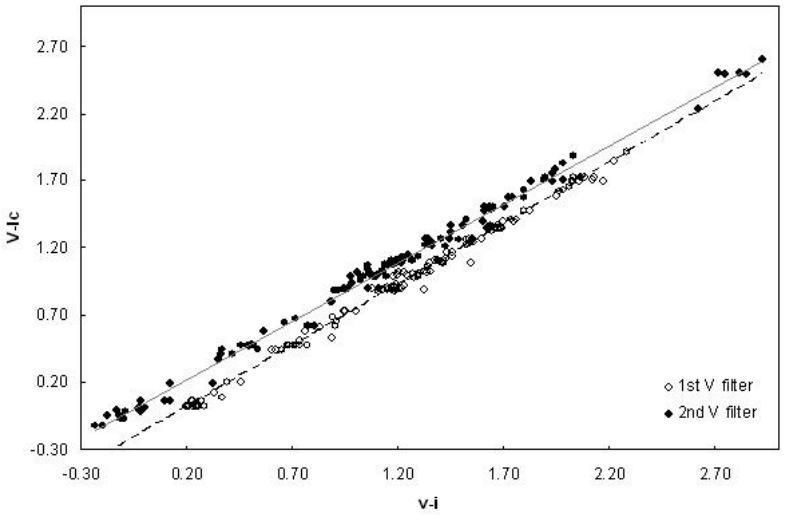

Figure 4. Transformation of $v–i$ to $V–I_C$ indices using standard stars (different V filters) indicating linearity over the range of $V–I_C$ measured.